Materials Science in Semiconductor Processing 13 (2010) 21–28

Contents lists available at ScienceDirect

Materials Science in Semiconductor Processing

journal homepage: www.elsevier.com/locate/mssp

Surfactant free hydrothermally derived ZnO nanowires, nanorods, microrods and their characterization

G. Nagaraju [a], S. Ashoka [a], P. Chithaiah [a], C.N. Tharamani [b], G.T. Chandrappa [a,*]

[a] Department of Chemistry, Central College Campus, Bangalore University, Bangalore, India
[b] Department of Chemistry, University of Saskatchewan, Saskatoon, Canada, SK S7N 5C9

ARTICLE INFO

Available online 26 February 2010

Keywords:
Surfactant
Hydrothermal
Nanorods
Nanowires
Microrods

ABSTRACT

ZnO nanowires, nanorods and microrods have been prepared by an organic-free hydrothermal process using $ZnSO_4$ and $NaOH/NH_4OH$ solutions. The powder X-ray diffraction (PXRD) patterns reveal that the ZnO nano/microrods are of hexagonal wurtzite structure. The Fourier transform infrared (FT-IR) spectrum of ZnO powder shows only one significant spectroscopic band at around 417 cm^{-1} associated with the characteristic vibrational mode of Zn–O bonding. The thickness 75–300 nm for ZnO nanorods and 0.2–1.8 μm for microrods are identified from SEM/TEM images. UV–visible absorption spectra of ZnO nano/microrods show the blue shift. The UV band and green emission observed in photoluminescence (PL) spectra are due to free exciton emission and singly ionized oxygen vacancy in ZnO. Finally, the mechanism for organic-free hydrothermal synthesis of the ZnO nano/microrods is discussed.

1. Introduction

In recent years, nanostructural materials having high surface to volume ratio are of great consideration in the light of their significant potential applications in electronics, optoelectronics and catalysis [1]. Due to decrease in particle size, more and more novel properties resulting from quantum effects have been observed [2]. Nanocrystalline metal oxides play a very important role in many areas of chemistry, physics and materials science. These can adopt a vast number of structural geometries with an electronic structure that can exhibit metallic, semiconductor or insulator characteristics [3]. Binary oxides such as ZnO, CdO, SnO_2 and In_2O_3 have distinctive properties and are now widely used as transparent conductive oxide materials and gas sensors [4]. These oxides have two unique structural features: mixed cation valencies and an adjustable oxygen deficiency, which are the bases for creating and tuning many novel materials properties [5]. ZnO is a well-known n-type wide band gap semiconductor (E_g=3.37 eV) with a large exciton binding energy of 60 meV [6]. As a result the material is transparent to visible light but not to UV light. Furthermore, ZnO is biocompatible and it exhibits both piezo- and pyroelectric properties [7]. ZnO is one of the 'hardest' materials in the II–VI compound family. As a result, ZnO devices do not suffer from dislocation degradation during operation [8]. ZnO with various morphologies such as nanowires, nanorods, nanobelts, nanotubes and nanotetrapods [9–11] have been prepared by a number of methods. Recent examples of the utilization of ZnO nanorods are found in hybrid and dye-sensitized solar cells, field-emitting cathodes, chemical sensors, low-voltage and short-wavelength electro-optical devices such as light emitting diodes and diode lasers, surface acoustic wave filters and varistors [12–18], etc. ZnO is a potential sensor of NH_3 and a photocatalyst to reduce the emission of NO_x. Due to higher solubility of ZnO in water, conventional synthesis of nanostructural materials has been considered to be especially difficult in the absence of

* Corresponding author. Tel.: +9180 22961350.
E-mail address: gtchandrappa@yahoo.co.in (G.T. Chandrappa).

1369-8001/$ - see front matter © 2010 Elsevier Ltd. All rights reserved.
doi:10.1016/j.mssp.2010.02.002

any organics [14]. Template assisted sol–gel process, solvothermal, thermal evaporation, metal organic chemical vapour deposition, spray pyrolysis and microwave techniques are some of the other synthetic routes used [13,14,19–21]. Recently, ZnO nanorods are synthesized by the hydrothermal method using zinc chloride with 25% ammonia [22]. Ken Elen et al. [7] explained the various parameters in view of reducing the diameter of the ZnO nanorods synthesized by the hydrothermal method. They considered 2^{8-4} fractional factorial design of experiment which is applied to identify the important parameters that affect the average diameter of ZnO rods. The absence of an additive simplifies the procedure and the use of water as the reaction medium makes the process ecologically less demanding. Hydrothermal synthesis is becoming popular for environmental reason, since water is used as a reaction solvent than organics. This method has been widely used to prepare nanomaterials due to its simplicity, high efficiency and low cost.

Herein, we report the preparation of ZnO nano/microrods by an organic-free hydrothermal method. In order to understand the behavior of 1-D ZnO nano/microrods; the effects of mineralizer, temperature, concentration of the starting solution and the treatment time on their morphology have been investigated. The effect of particle size on the intensity of PL spectra at room temperature is investigated.

2. Experimental details

In a typical hydrothermal process [23–25], 1 g $ZnSO_4 \cdot 7H_2O$ (3.47 mmol) is dissolved in 25 ml of distilled water. To this, 10 ml of 2 M NaOH aqueous solution is introduced resulting in the formation of white precipitate. The white precipitate is stirred for 5 min with a magnetic stirrer and transferred into Teflon-lined stainless steel autoclaves with a capacity of 25 ml, sealed and maintained at different temperatures (180–200 °C) for several hours (6–24 h). Similar experiments are carried out using ammonia solution instead of NaOH. To this solution, ammonium hydroxide is added drop by drop to adjust the pH value of the solution. A white precipitate is obtained when the pH of the solution reaches 9. The obtained product is retrieved from the solution by centrifugation and washed with distilled water followed by ethanol and finally dried in air.

Zinc sulphate and sodium hydroxide are purchased from E. MERCK chemicals. Powder X-ray diffraction (XRD) data are recorded in θ–2θ coupled mode on Philips X'pert PRO X-ray diffractometer using graphite monochromatized Cu Kα radiation (λ=1.541 Å).The Fourier transform infrared spectrum of the sample is collected using Thermo Nicollet FT-IR spectrometer. The absorption spectra of the samples are measured on a UV-3101 Shimadzu visible spectrometer. Scanning electron micrograph images are taken with JEOL (JSM-840A) scanning electron microscope (SEM). Transmission electron microscopy (TEM) images are observed with a JEOL 100 CX electron microscope. Photoluminescence studies are carried out on a Perkin-Elmer LS-55 luminescence spectrometer using Xe lamp with an excitation wavelength of 325 nm at room temperature.

3. Results and discussion

Fig. 1 shows the powder XRD patterns of the samples prepared at 180–200 °C for 6–20 h. All the diffraction peaks in the pattern can be indexed as the pure hexagonal phase of ZnO with space group $P6_3mc$. These peaks are free from $Zn(OH)_2$ impurities within the detection limit of the XRD technique. This indicates that sample is composed of wurtzite structural ZnO with the lattice constants a=3.249 and c=5.206 Å which are consistent with the values in the standard card (JCPDS 36-1451).

Fig. 2 shows the FT-IR spectrum of ZnO nanorods in the range 2000–300 cm^{-1}. There is only one significant spectroscopic band around 417 cm^{-1} associated with the characteristic vibrational mode of Zn–O bonding [26]. UV–visible spectra of the ZnO nanorods (Fig. 3(a)) and microrods (Fig. 3(b)) prepared at 200 and 180 °C for 20 h using NaOH exhibits a strong absorption between 362 and 371 nm which corresponds to a band gap of 3.43 and 3.34 eV. It is known that bulk ZnO (3.2 eV) has absorption at 387 nm in the UV–visible spectrum and is

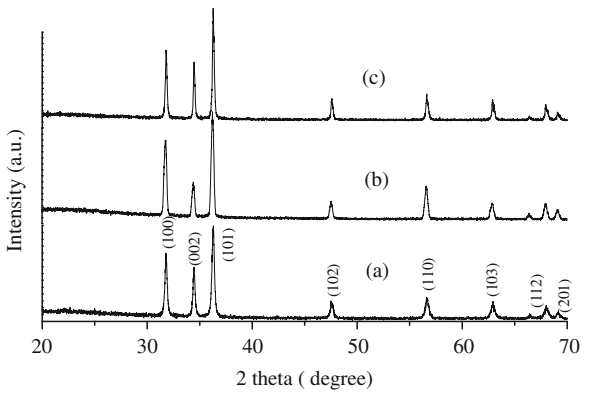

Fig. 1. Powder XRD patterns of ZnO nano/microrods prepared at (a) 180 °C for 6 h using NH_4OH; (b) 180 °C for 20 h using NaOH and (c) 200 °C for 20 h using NaOH.

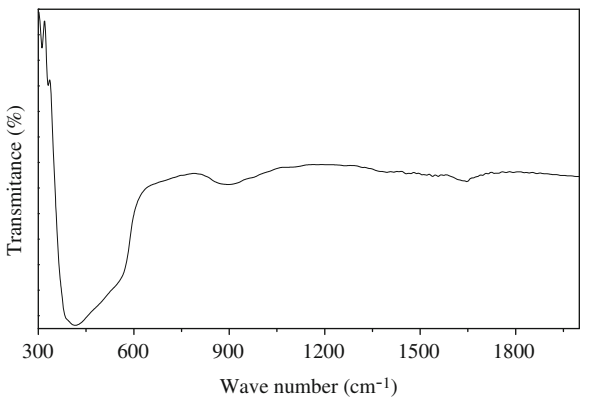

Fig. 2. FTIR spectrum of ZnO nanorods prepared at 200 °C for 20 h using NaOH.

obviously larger than the as-prepared ZnO nanorods (362 nm) and microrods (371 nm). Compared to the bulk ZnO, the observed blue shift in ZnO nanorods and microrods may be due to the size effect [27].

Fig. 4 shows SEM images of ZnO nano/microrods prepared using NaOH as mineralizer at 180–200 °C for 6–20 h. By controlling the experimental conditions (temperature and duration), we have successfully prepared ZnO nano/microrods of various morphologies through the hydrothermal method. Fig. 4(a) shows the low magnification image of the multipods or star-like morphologies. Inset of Fig. 4(a) reveals that the number of arms from 5 to 10 have a common origin with almost equal length and thickness of about 150–400 nm. Each multipod or star-like morphology is composed of sub-micrometer sized rods which form radiating structures [28]. One can also feel that these star-like particles or intertwined ellipsoid or intertwined needles depending on the lengths of the branches which are formed at 180 °C for 6 h. The formation of star-like structures may be explained by the coalescence of several nuclei [29]. The growth of these star-like ZnO particles does not follow the simple LaMer and Dinegar theory [30], as it appears that there are several nucleation events. Den Ouden and Thompson have shown that monodisperse populations can form even though nucleation extends over a period of time, if the particle growth is slow relative to nucleation. After the first nucleation, the particles begin to grow by diffusion of the reactants through solution to the surface of the growing particles [31]. As the hydrothermal duration increases, the as-obtained product is still retained its morphology, but further nucleation occurs leading to the formation of microrods. ZnO microrods (Fig. 4b) of about 0.6–1.8 μm in thickness and 3–11 μm in length having hexagonal cross-section with sharp edges and tips are formed at 180 °C for 20 h. Such hexagonal morphology is consistent with the idealized growth behavior of the ZnO crystal described by Laudise and Ballman [32] who deemed that ZnO prefer to grow along the [0 0 0 1] direction. The crystal facet with faster growth velocity tends to disappear and the facet

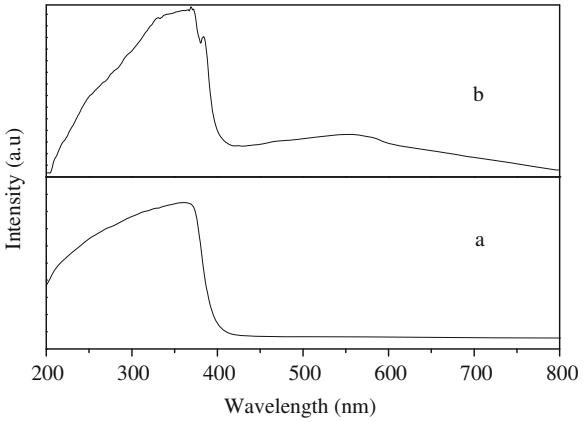

Fig. 3. UV–visible spectra of ZnO (a) nanorods prepared at 200 °C for 20 h and (b) microrods prepared at 180 °C for 20 h using NaOH.

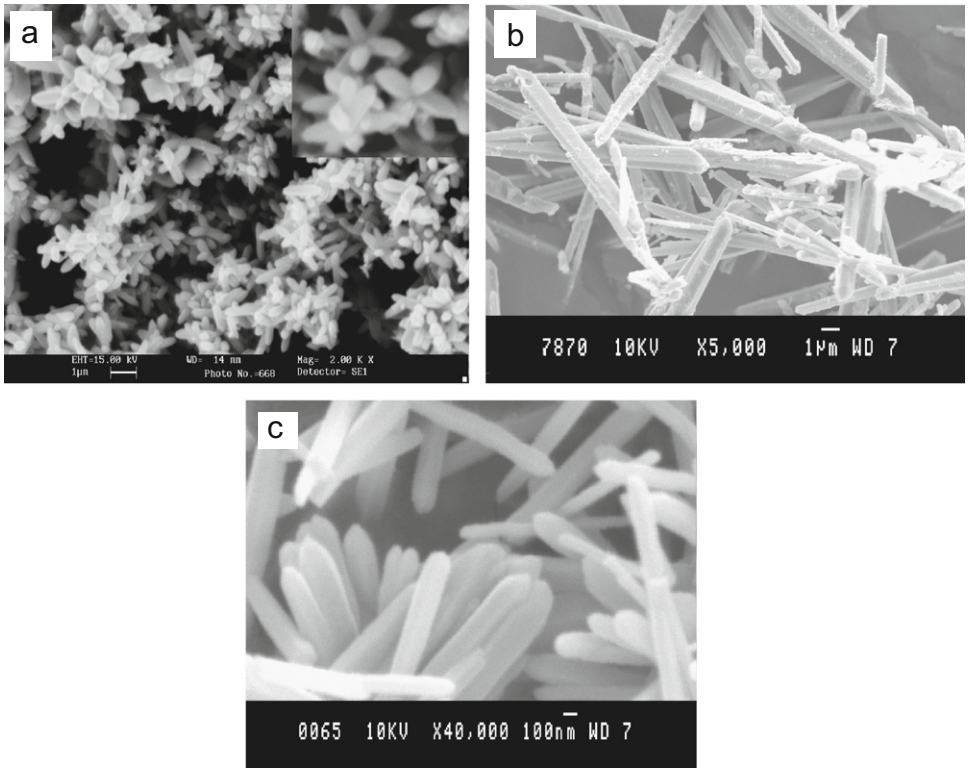

Fig. 4. SEM images of ZnO nano/microrods prepared using NaOH at (a) 180 °C for 6 h; (b) 180 °C for 20 h and (c) 200 °C for 20 h.

with slower growth velocity is prone to remain. Hence sharp tips are formed during the nano/microrods growth. In particular, these results can usually be found in the synthesis of nano/microrods with monoclinic and hexagonal phase [33]. Increasing the hydrothermal treatment temperature to 200 °C for 20 h resulted in the production of smooth surface hexagonal cross nanorods (Fig. 4c) with sharp tips having a thickness of about 150 nm and several micrometers in length. It was also found that the assembly pattern of ZnO architectures became looser with the prolonging of reaction time. i.e., assembly structure of original ZnO products which were formed quickly in the beginning of the reaction temperature [34].

Fig. 5 reveals SEM images of the samples prepared at 180 °C for 6–24 h using NH_4OH as mineralizer. The thickness of the microrods (Fig. 5(a)–(c)) is in the range 0.2–1.8 μm and the length is about 1.8–6.2 μm. When the growth time is increased to 24 h, flake-like structures were observed (Fig. 5(d)). It is interesting to note that the diameter of the rods is reduced by decreasing the concentration of $ZnSO_4$ (0.347 mmol) and increasing the temperature. SEM images (Fig. 6a) show that the products prepared at 200 °C for 6 h are composed of ZnO multipod structures, appears like flowers in which each pod radially grows from one center. The thickness of each rod is almost uniform along its length and the typical thickness of the rod range from 75 to 150 nm and length of each rod is about 0.5–2.5 μm. Fig. 6(b) shows large quantities of ZnO nanowires prepared at 200 °C for 20 h with very high aspect ratio. Thicknesses of the nanowires vary from 70 to 140 nm and several micrometers in length are observed.

The EDS/TEM sample of ZnO nanorods prepared at 200 °C for 20 h (concentration of $ZnSO_4$ is 0.347 mmol) is shown in Fig. 7, which is the direct evidence that led to the conclusion that except Zn and O (elements of ZnO), no other elements existed. The copper peak in the spectrum is attributed to the copper meshes of the TEM grid. The morphology and structure of individual ZnO nanorods have been characterized with further detail using TEM, which are shown in Fig. 8. Fig. 8(a) shows that nanowires are straight and uniform along their entire length. From Fig. 8(b), it can be seen that an end of the ZnO nanowires is pointed like a sword with thickness of about 50–100 nm. The SAED dot pattern (Fig. 8(c)) indicates that the nanorods are single crystal in nature and can be indexed as hexagonal ZnO phase which is in accord with the XRD results in Fig. 1.

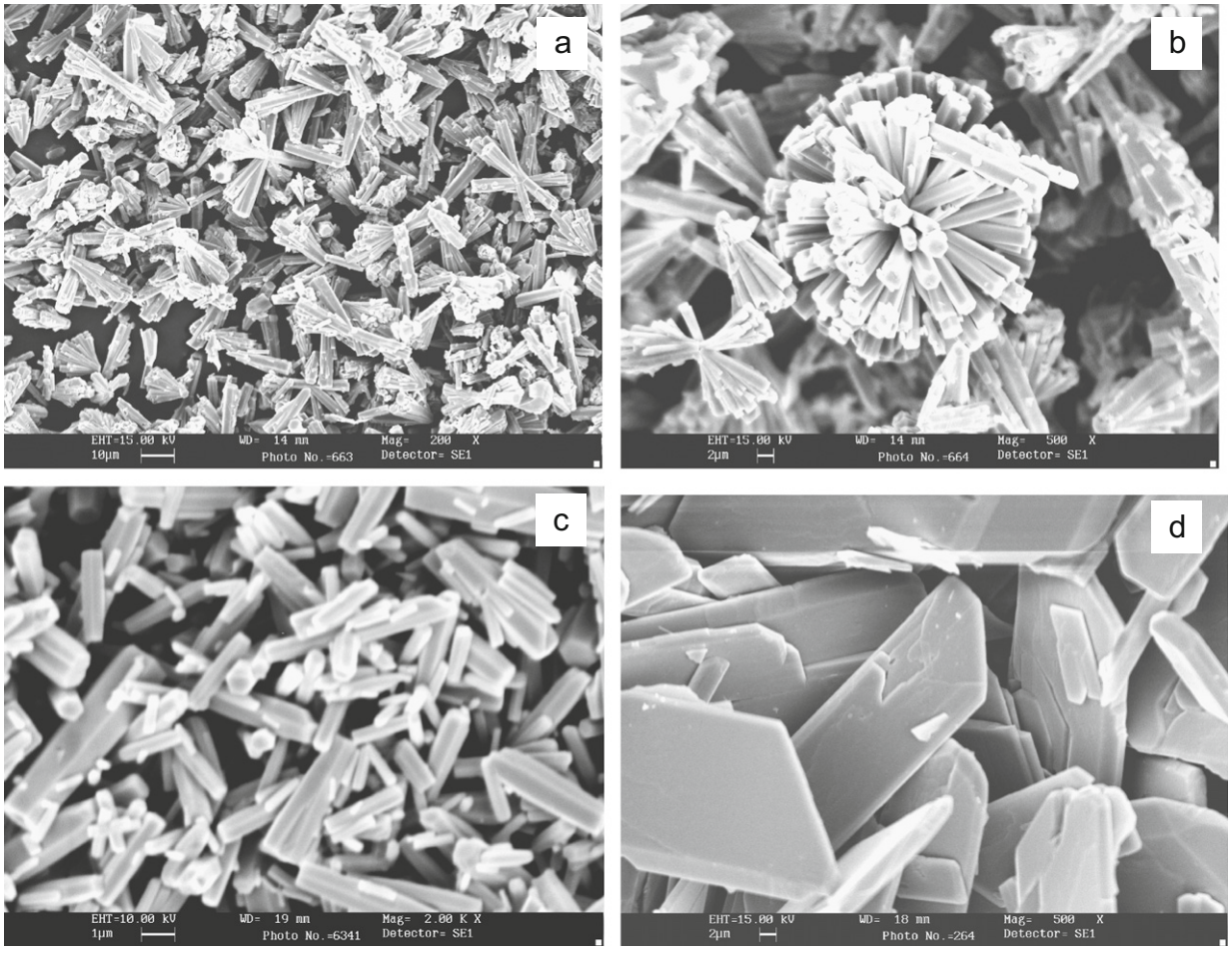

Fig. 5. SEM images of the ZnO microrods/flakes prepared using NH_4OH at 180 °C for (a, b) 6 h; (c) 20 h and (d) 24 h.

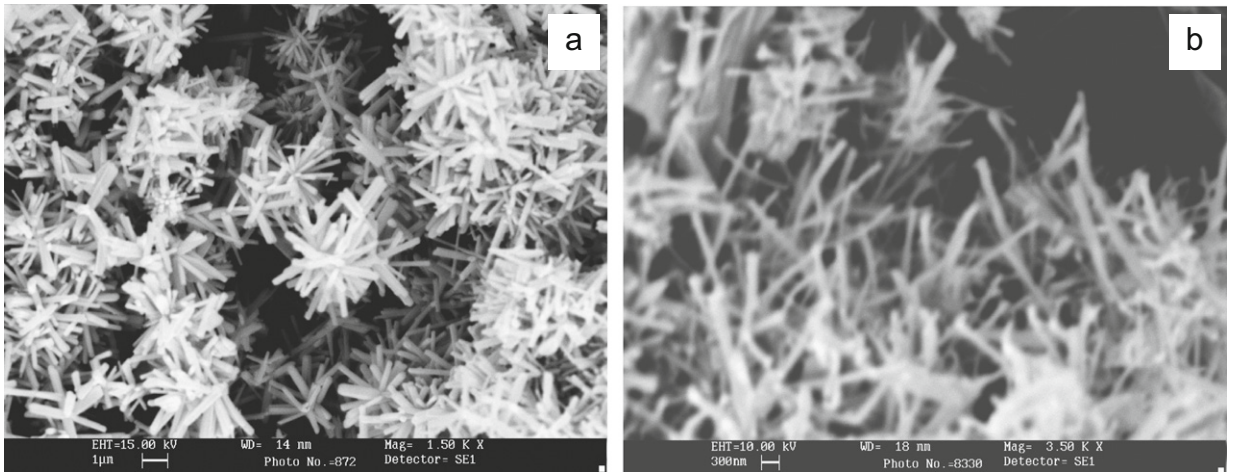

Fig. 6. SEM images of the ZnO nanorods/wires prepared in low concentration (0.347 mmol) using NaOH at 200 °C for (a) 6 h and (b) 20 h.

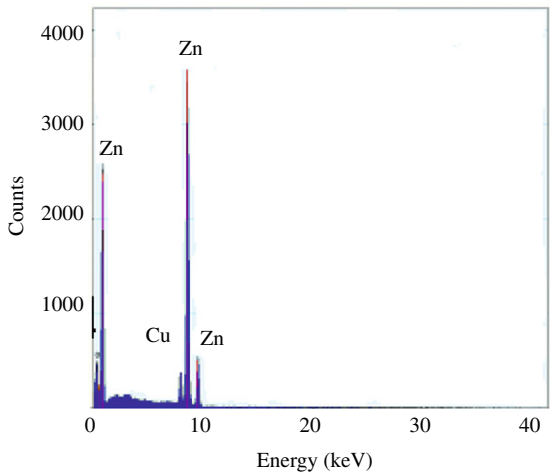

Fig. 7. EDS spectrum of ZnO nanorods prepared at 200 °C for 20 h.

Laudise and Ballman [32] and Laudise et al. [35] were the first to describe the idealized growth habit of a ZnO crystal, prepared by the hydrothermal method in an alkaline medium. A possible growth mechanism for the formation of the nano/microrods can be explained on the basis of the polar structure of ZnO. ZnO exhibits a hexagonal wurtzite structure consisting of planes of tetrahedrally coordinated O^{2-} and Zn^{2+} ions, stacked alternately along the polar *c*-axis. The tetrahedral coordination in ZnO results in piezoelectric and pyroelectric properties due to the absence of inversion symmetry. The oppositely charged ions produce positively charged Zn-(0 0 0 1) and negatively charged O-(0 0 0–1) surfaces, resulting in a normal dipole moment and spontaneous polarization along the *c*-axis as well as a variance in surface energy [36]. In the hydrothermal process, the growth unit of ZnO is $[Zn(OH)_4]^{2-}$, which leads to the different growth rate of planes shown in the following: $V(0\,0\,0\,1) > V(0\,1\text{–}1\,0) > V(0\,0\,0\,1)$. As we know, more rapid the growth rate is, quicker the disappearance of the plane. Therefore, the (0 0 0 1) plane, the most rapid growth rate plane disappears in the hydrothermal process, which leads to the pointed shape in an end of the *c*-axis. However, the plane, the slowest growth rate plane, is maintained in the hydrothermal process, which leads to the plain shape in another end of the *c*-axis [1,28,37,38]. The idealized growth habit of ZnO [39] is as shown in Fig. 9.

In principle, the crystal growth process includes nuclei and growth units. In our experiment due to different pH values, the quantity of $Zn(OH)_2$ and of the growth unit $[Zn(OH)_4]^{2-}$ which contribute, respectively, to the nucleation and growth of ZnO are also different in the aqueous solution. Based on the well known behavior of Zn in alkaline media, we presume that when the pH value is equal to 11 using NaOH as mineralizer, a small quantity of $Zn(OH)_2$ and a large quantity of growth unit $[Zn(OH)_4]^{2-}$ are obtained [40]. Thus in the hydrothermal process, the quantity of the corresponding ZnO nuclei is smaller. Therefore, there is enough growth unit $[Zn(OH)_4]^{2-}$ to make ZnO nanorods grow from the circumference of the ZnO nuclei. In this experiment, OH^- is first introduced into Zn^{2+} aqueous solution, and then $Zn(OH)_2$ colloids formed, according to the reaction

$$Zn^{2+}_{(aq)} + 2OH^- \leftrightarrow Zn(OH)_{2(s)} \quad (1)$$

If the pH value in the aqueous solution is about 11, $Zn(OH)_2$ is the main composition. During the hydrothermal process, part of the $Zn(OH)_2$ colloids dissolves into Zn^{2+} and OH^-. When the concentration of Zn^{2+} and OH^- reaches the super-saturation degree of ZnO. ZnO nuclei is formed according to reaction 4. Thus, the growth units of $[Zn(OH)_4]^{2-}$ formed [1,40] according to reaction 3. The possible reaction mechanism is

$$Zn(OH)_2 \rightarrow Zn^{2+} + 2OH^- \quad (2)$$

$$Zn(OH)_2 + 2OH^- \leftrightarrow [Zn(OH)_4]^{2-} [Zn(OH)_4]^{2-} \leftrightarrow Zn^{2+} + 4OH^- \text{ (dissolution)} \quad (3)$$

$$Zn^{2+}_{(aq)} + 2OH^- \rightarrow ZnO_{(s)} + H_2O \text{ (nucleation)} \quad (4)$$

As the hydrothermal treatment temperature reaches 200 °C, in addition to pH factor (i.e. nuclei and growth

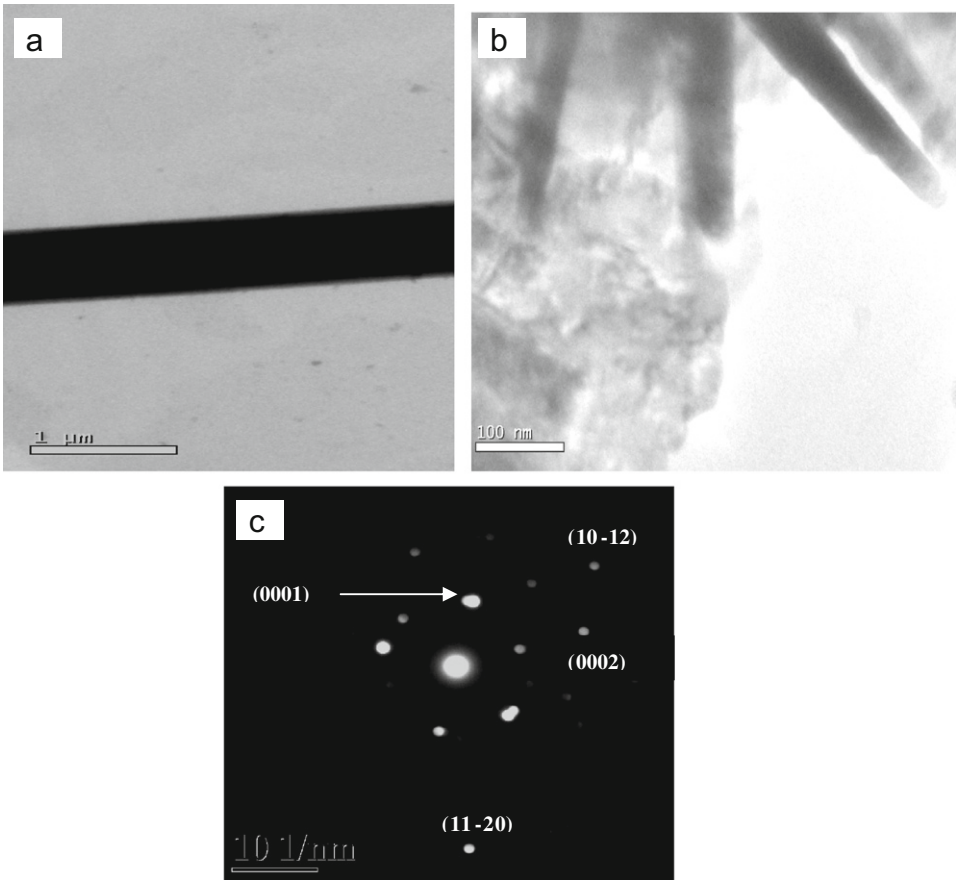

Fig. 8. TEM images of the single ZnO nanowire prepared in low concentration (0.347 mmol) using NaOH at 200 °C for 20 h.

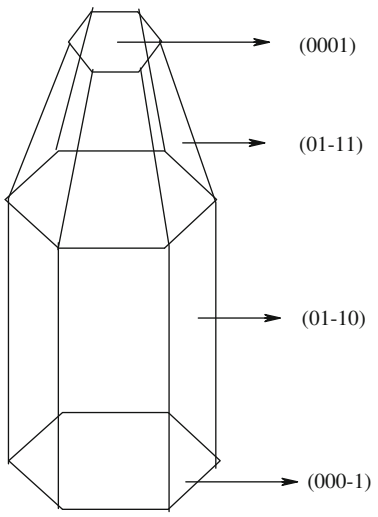

Fig. 9. Idealized growth habit of the ZnO crystal.

unit), active sites are generated around the circumference of ZnO nuclei, so that the ZnO will preferentially grown on the active sites along the (0001) direction [41]. The mechanism is illustrated in Fig. 10.

In the case of ammonia as a mineralizer, the pH value is equal to 9. Larger quantity of growth unit $Zn(OH)_2$ and a smaller quantity of $[Zn(NH_3)_4]^{2+}$ are obtained. During the hydrothermal treatment, even if $[Zn(NH_3)_4]^{2+}$ decompose to free Zn^{2+}, the quantity of growth unit $[Zn(OH)_4]^{2-}$ is not enough. Therefore, microrods are formed [22,40]. The possible reaction mechanism is

$$Zn^{2+} + 4NH_3 \cdot H_2O \rightarrow [Zn(NH_3)_4]^{2+} + H_2O_{(s)}[Zn(NH_3)_4]^{2+} + 2OH^- \rightarrow ZnO + 4NH_3 + H_2O \quad (5)$$

In order to assess the crystalline quality and investigate the optical properties of the nanorods, PL spectra are taken using Xe lamp as the excitation source of 325 nm. Figs. 11 and 12 show PL spectra of the samples prepared at different conditions. Fig. 11(a) and (c) shows strong UV emission at 398 nm and Figs. 11(b), 12(a)–(c) show strong violet emission at 403–405 nm. The emission in the UV region is attributed to the recombination between electrons in the conduction band and holes in the valence band [42]. Violet emission is attributed to the exciton transition [43]. The weak green band emission at 484 nm corresponds to the singly ionized oxygen vacancy in ZnO and this emission results from the recombination of a photogenerated hole with the singly ionized charge state of the specific defect. Oxygen vacancies have been considered as the most common defects and usually act as radiative centers in luminescence process. In addition, ZnO nanocrystals with high aspect ratio should also favor the existence of large

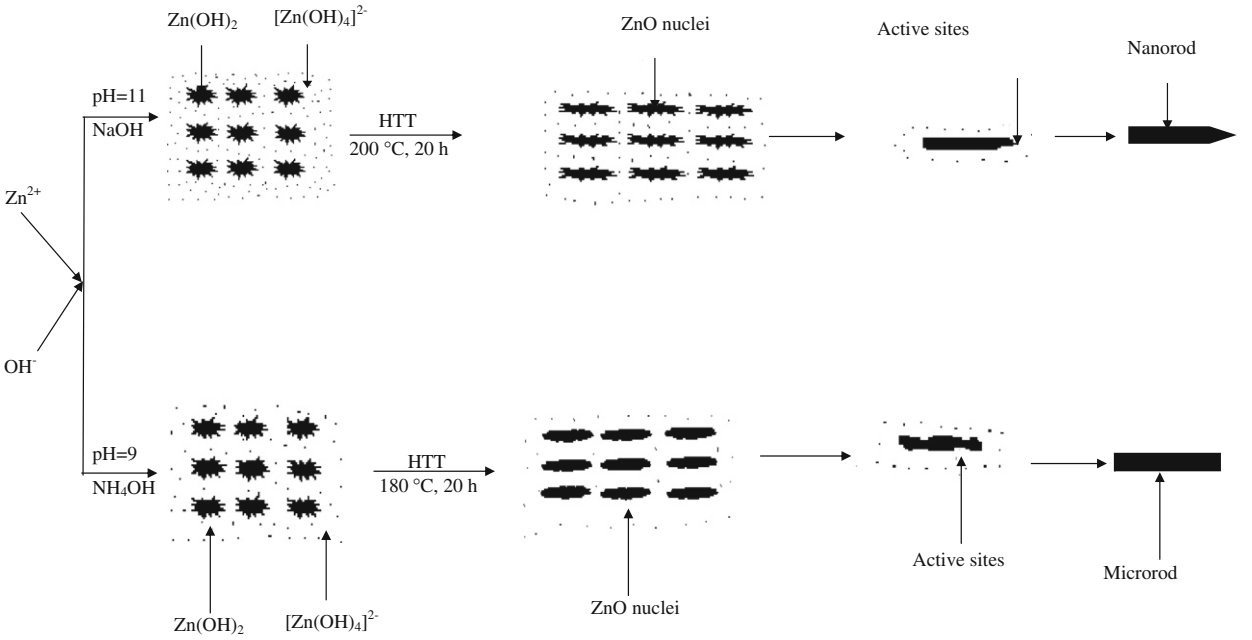

Fig. 10. Schematic growth diagram of ZnO nano/microrods prepared by surfactant-free hydrothermal process.

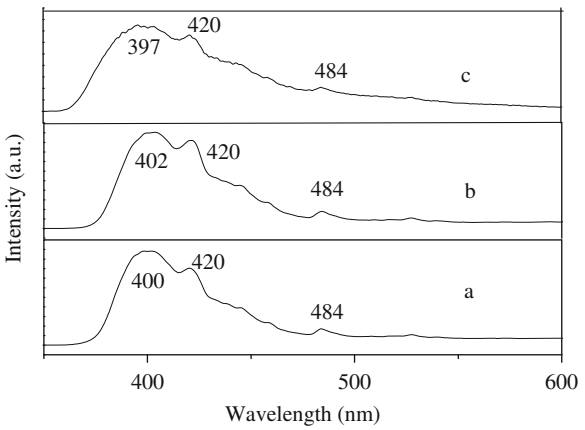

Fig. 11. Photoluminescence spectra of ZnO nano/microrods using NaOH at (a) 180 °C for 6 h; (b) 180 °C for 20 h and (c) 200 °C for 20 h.

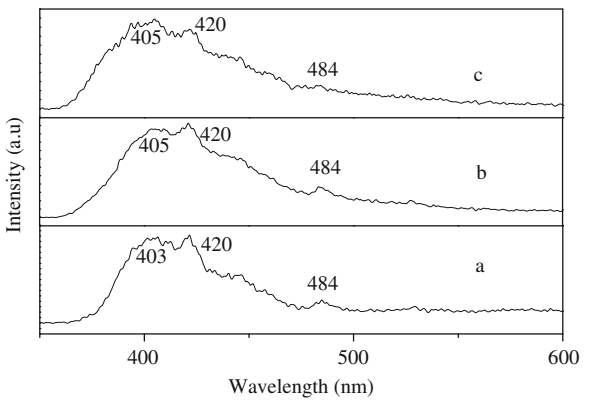

Fig. 12. Photoluminescence spectra of ZnO microrods/flakes using NH_4OH at 180 °C for (a) 6 h; (b) 20 h and (c) 24 h.

quantities of oxygen vacancies. The strong UV emission and weak green emission in PL spectra indicate that the ZnO nano/microrods have a good optical quality with few oxygen vacancies [44]. Blue emission at 421 nm is electron transition from the shallow donor level of Zn interstitials to the valence band. The excellent room temperature UV emission property should be attributed to the high purity and perfect crystallinity of the as-synthesized ZnO nanorods. Therefore, the obtained ZnO nanorods are promising as a high performance optical material.

4. Conclusions

In summary, by means of an organic-free hydrothermal process, ZnO nanowires, nanorods and microrods with the hexagonal structure have been prepared. It is found that nature of the mineralizer, reaction temperature and treatment time have significant influence on the morphology of ZnO nanowires, nanorods and microrods. Powder XRD results show that the nano/microrods are hexagonal and single crystal in nature. SEM/TEM images reveal that the thickness of the nanowires/rods is in the range 75–300 nm and microrods are in the range 0.2–1.8 μm. It was interesting to note that the nanorods had grown from one center to form radial clusters, which consist of more than four rods grown from the center at different directions. The sample prepared at 200 °C for 20 h shows a smooth polished surface. It is possible to reduce the thickness of the ZnO rods by decreasing the concentration and increasing the temperature. UV–visible spectra of the ZnO nanorods and microrods show blue shift compared to bulk ZnO. The PL spectra of the ZnO

nanorods consist of an intense UV emission at 398 nm and microrods possess violet emissions at 405 nm.

Acknowledgements

The author G.T. Chandrappa is thankful to the Department of Science and Technology, NSTI Phase-IV, New Delhi, Government of India for the financial support to carryout this research. We also thank Prof. Sarala Upadhya, Department of Mechanical Engineering, UVCE, Bangalore University for her help in recording SEM images.

References

[1] Zhang H, Yang D, Ji Y, Ma X, Xu J, Que D. J Phys Chem B 2004; 108:3955.
[2] Zhang H, Yang D, Li S, Ma X, Ji Y, Xu J, et al. Mater Lett 2004; 59:1696.
[3] Garcia MF, Arias MA, Hanson JC, Rodriguez JA. Chem Rev 2004;104:4063.
[4] Ginley DS, Bright C. Mater Res Soc Bull 2000;25:15.
[5] Wang ZL. Adv Mater 2003;15:432.
[6] Zhang BP, Binh NT, Wakatsuki K, Segawa Y, Kashiwaba Y, Haga K. Nanotechnology 2004;15:S382.
[7] Elen K, Rul HV, Hardy A, Van Bael MK, Haen JD, Peeters D, et al. Nanotechnology 2009;20:055608.
[8] Xia LL, Xin TQ, Lu SC, Chun LY. Chin Phys Lett 2005;22:998.
[9] Huang MH, Wu Y, Feick H, Tran N, Weber E, Yang P. Adv Mater 2001;13:113.
[10] Guo L, Ji YL, Xu H. J Am Chem Soc 2002;124:14864.
[11] Lepot N, Van Bael MK, Van den Rul H, Haen JD, Peeters R, Franco D, et al. Mater Lett 2007;61:2624.
[12] Lao JY, Wen JG, Ren ZF. Nano Lett 2002;2:1287.
[13] Heo YW, Norton DP, Tein LC, Kwon Y, Kang BS, Ren F, et al. Mater Sci Eng R 2004;47:1.
[14] Ozgur U, Alivov Y, Liu C, Teke A, Reshchikov MA, Dogan S, et al. J Appl Phys 2005;98:041301.
[15] Law M, Greene LE, Johnson JC, Saykally R, Yang PD. Nat Mater 2005;4:455.
[16] Kim DH, Jang HS, Lee SY, Lee HR. Nanotechnology 2004;15:1433.
[17] Wang CH, Chu XF, Wu MW. Sensors Actuators B 2006;113:320.
[18] Park WI, Kim JS, Yi GC, Bae MH, Lee HJ. Appl Phys Lett 2004; 85:5052.
[19] Vayssieres L. Adv Mater 2003;15:464.
[20] Audebrand N, Auffredic JP, Louer D. Chem Mater 1998;10:2450.
[21] Wang ZL. J Phys Condens Matter 2004;16:R829.
[22] Xu CX, Wei A, Sun XW, Dong ZL. J Phys D Appl Phys 2006;39: 1690.
[23] Chandrappa GT, Steunou N, Livage J. Nature 2002;416:702.
[24] Nagaraju G, Thipperudraiah KV, Chandrappa GT. Mater Res Bull 2008;433:297.
[25] Nagaraju G, Tharamani CN, Chandrappa GT, Livage J. Nanoscale Res Lett 2007;2:461.
[26] Gu F, Wang SF, Lu MK, Zhou GJ, Xu D, Yuan DR. Langmuir 2004;20:3528.
[27] Wang C, Shen E, Wang E, Gao L, Kang Z, Tian C, et al. Mater Lett 2005;59:2867.
[28] Krishnan D, Pradeep T. J Cryst Growth 2009;311:3889.
[29] Ruth A, McBride, Kelly JM, McCormack DE. J Mater Chem 1996;13:1196.
[30] LaMer V, Dinegar RH. J Am Chem Soc 1950;72:4847.
[31] Zou G, Li H, Zhang Y, Xiong K, Qian Y. Nanotechnology 2006;17:S313.
[32] Laudise RA, Balmann AA. J Phys Chem 1960;64:688.
[33] Wen F, Li W, Moon J, Kim JH. Solid State Commun 2005;135:34.
[34] Zuo A, Hu P, Bai L, Yuan F. Nanoplates Cryst Res Technol 2009;44:613.
[35] Laudise RA, Kolb ED, Caporaso AJ. J Am Ceram Soc 1964;47:9.
[36] Wang ZL. Mater Sci Eng R 2009;64:33.
[37] Komarneni S, Bruno M, Mariani E. Mater Res Bull 2000;35:1843.
[38] Yadav RS, Pandey AC. Physica E 2008;40:660.
[39] Li WJ, Shi EW, Zhong WZ, Yin ZW. J Cryst Growth 1999;203:186.
[40] Zhang H, Yang D, Ma X, Ji Y, Xu J, Que D. Nanotechnology 2004; 15:622.
[41] Gao P, Ying C, Wang S, Ye L, Guo Q, Xie Y. J Nanoparticle Res 2006;8:131.
[42] Wang J, Gao L. J Mater Chem 2003;13:2551.
[43] Monticone S, Tufeu R, Kanaev AV. J Phys Chem B 1998;102:2854.
[44] Fang Z, Tang K, Shen G, Chen D, Kong R, Lei S. Mater Lett 2006;60:2530.